A Birefringence Study of Changes in Myosin Orientation during Relaxation of Skinned Muscle Fibers Induced by Photolytic ATP Release

M. Peckham,* M. A. Ferenczi,‡ and M. Irving*

*The Randall Institute, King's College London, 26–29 Drury Lane, London WC2B 5RL, and ‡National Institute for Medical Research, Mill Hill, London NW7 1AA

ABSTRACT The birefringence of isolated skinned fibers from rabbit psoas muscle was measured continuously during relaxation from rigor produced by photolysis of caged ATP at sarcomere length 2.8–2.9 μm, ionic strength 0.1 M, 15°C. Birefringence, the difference in refractive index between light components polarized parallel and perpendicular to the fiber axis, depends on the average degree of alignment of the myosin head domain with the fiber axis. After ATP release birefringence increased by 5.8 ± 0.7% (mean ± SE, $n = 6$) with two temporal components. A small fast component had an amplitude of 0.9 ± 0.2% and rate constant of 63 s^{-1}. By the completion of this component, the instantaneous stiffness had decreased to about half the rigor value, and the force response to a step stretch showed a rapid (~1000 s^{-1}) recovery phase. Subsequently a large slow birefringence component with rate constant 5.1 s^{-1} accompanied isometric force relaxation. Inorganic phosphate (10 mM) did not affect the fast birefringence component but accelerated the slow component and force relaxation. The fast birefringence component was probably caused by formation of myosin.ATP or myosin.ADP.Pi states that are weakly bound to actin. The average myosin head orientation at the end of this component is slightly more parallel to the fiber axis than in rigor.

INTRODUCTION

Muscle contraction involves a cyclical interaction of the myosin head domain with the actin filament, driven by the free energy of ATP hydrolysis. Little is known about structural changes in myosin and actin during the ATP hydrolysis cycle, but it is generally assumed that a structural change in the myosin-actin complex is directly responsible for the generation of force and shortening. To investigate this in a working muscle fiber it is useful to synchronize the ATP hydrolysis cycles in the myosin population. One way to achieve this is to release ATP in a rigor muscle fiber by flash photolysis of a biologically inactive ATP precursor, caged ATP (Goldman et al., 1982, 1984). This approach has been used successfully to investigate mechanico-chemical coupling in muscle (reviewed by Hibberd and Trentham, 1986; Goldman, 1987). More recently it has been combined with structural methods including x-ray diffraction (Poole et al., 1988, 1991; Brenner et al., 1989), electron microscopy (Hirose et al., 1993), fluorescence polarization (Tanner et al., 1992; Allen et al., 1992), and birefringence (Ferenczi et al., 1986; Irving et al., 1988). These structural methods have different technical advantages and limitations and yield complementary information.

We used birefringence measurements to follow changes in the orientation of myosin heads after photolysis of caged ATP in isolated skinned muscle fibers. The birefringence is the difference in refractive index between light components polarized parallel and perpendicular to the muscle fiber axis. Fiber birefringence is higher in relaxing conditions (in the presence of ATP but without calcium) than in rigor (Taylor, 1976; Peckham and Irving, 1989). This birefringence difference is caused by a change in the average degree of alignment of the myosin head domain with the fiber axis (Irving et al., 1988; Haskell et al., 1989; Peckham and Irving, 1989). The long axis of the myosin head is more parallel to the fiber axis in relaxing than in rigor conditions.

Birefringence was determined from continuous measurements of optical retardation, which is the phase difference between parallel and perpendicular polarized light components that is introduced by the fiber. The retardation is equal to the birefringence multiplied by the optical path length in the fiber. The latter is sensitive to changes in the cross-sectional shape of the fibers, which can be made acceptably small by careful selection and mounting of the fibers and by working at sarcomere lengths at which there is a small amount of resting tension (Irving, 1993). The present measurements were all made at a sarcomere length of 2.8–2.9 μm. Birefringence is sensitive to changes in the volume of the filament lattice (Fredericq and Houssier, 1973; Peckham and Irving, 1989), as well as to changes in myosin orientation. Volume changes associated with ATP release were minimized by using propionate-based solutions with an ionic strength of 0.1 M (Brenner et al., 1984; Ferenczi et al., 1987; Peckham and Irving, 1989). With these precautions to minimize other contributions to the recorded retardation signals, the latter can provide a continuous measure of the change in myosin head orientation in a single muscle fiber during the relaxation induced by photolytic release of ATP.

Received for publication 15 November 1993 and in final form 8 June 1994.

Address reprint requests to Malcolm Irving, The Randall Institute, King's College London, 26–29 Drury Lane, London, WC2B 5RL, UK. Tel.: 44 71 836 8851; Fax: 44 71 497 9078; E-mail: udbp075@bay.cc.kcl.ac.uk.

0006-3495/94/09/1141/08 $2.00

MATERIALS AND METHODS

Bundles of chemically skinned fibers from rabbit psoas muscle were prepared as described by Peckham and Irving (1989) and stored in relaxing solution (Table 1) containing 50% glycerol at −20°C for up to two weeks before use. Segments of single fibers were dissected from the bundles in

TABLE 1 Solution compositions (mM)

	Na_2ATP	cATP	$MgCl_2$	[MgATP]	$[Mg^{2+}]$	KPr	EGTA	EDTA	Imid.	GLH	Pi
Relaxed	1.1	0.0	3.3	1.0	2.0	63.1	5.0	0.0	10.0	0.0	0.0
Rigor	0.0	0.0	0.0	0.0	0.0	73.6	2.5	2.5	10.0	0.0	0.0
Rigor + cATP	0.0	5.0	3.3	0.0	2.0	31.8	5.0	0.0	10.0	30.0	0.0
Rigor + cATP + Pi	0.0	5.0	4.0	0.0	2.0	11.5	5.0	0.0	10.0	30.0	10.0

Abbreviations used: cATP, caged ATP (P^3-1-(2-nitrophenyl)ethyl ester of adenosine 5'-triphosphate); Pr, propionate; Pi, inorganic phosphate; Imid., imidazole; GLH, reduced glutathione. Square brackets denote free concentrations of these species. All solutions have a calculated ionic strength of 100 mM, pH 7.0 at 15°C. The ionic strength and [Mg] calculation for the solutions containing cATP assumes that 1 mM ATP is released after photolysis.

relaxing solution at 10°C. The ends of a segment about 2 mm long were crimped in aluminium T-clips. The segment was transferred to the experimental chamber and attached via the T-clips to two stainless steel hooks dipping into the chamber. One of the hooks was attached to a motor (Ford et al., 1977) for controlling the segment length, the other to a force transducer (SensoNor AE801, Horten, Norway). The chamber was made by gluing a glass base and quartz sides onto two stainless steel tubes (~1 mm in diameter), the ends of which were ~6 mm apart. The muscle fiber was 100–200 μm from the quartz window facing the laser used for caged ATP photolysis (see below). The top of the chamber was covered with a glass coverslip. The solution bathing the fiber was exchanged by flushing through 100–200 μl of solution via the stainless steel tubes using inlet and waste syringes driven by stepper motors. The inlet tube was attached to a mixer to provide a choice of up to five solutions. The temperature of the bath was measured with a thermistor and controlled by a Peltier device; during the experiments the temperature was 15°C except where stated.

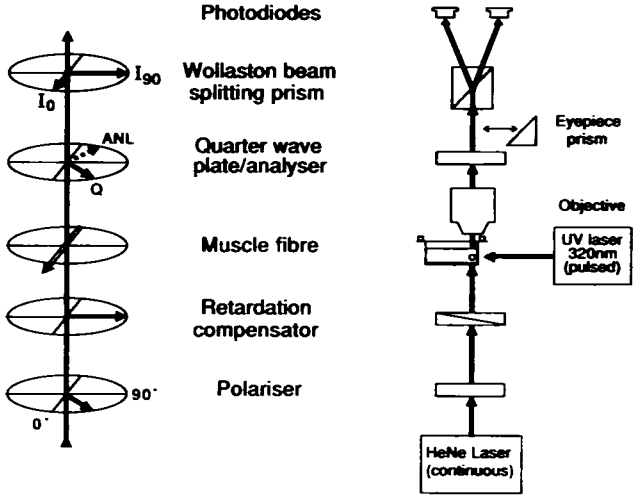

FIGURE 1 Schematic diagram of the optical apparatus used to measure muscle fiber retardation. Light from a 5 mW He-Ne laser was polarized at 45° to the muscle fiber axis by a dichroic sheet polarizer. A calibrated retardation was introduced by a Babinet-Soleil compensator (Halle, Berlin). Light transmitted by or bypassing the muscle fiber was collected by a water immersion objective (Nikon 10X, N.A. 0.22). For observing the fiber between crossed polarizers the analyzer (ANL) and eyepiece prism were inserted. For continuous retardation measurements the quarter-wave plate (Q), Wollaston beam-splitting prism and two photodiodes were used as described in the text. The left side shows polarization axes; labels 0° and 90° denote directions parallel and perpendicular to the fiber axis, respectively. The arrows in the horizontal plane denote transmission axes for polarizer, analyzer and Wollaston prism, and slow (larger retardation) axes for compensator, muscle fiber and quarter-wave plate. Spherical lenses (not shown) formed an image of an adjustable slit at the fiber, and an image of the back focal plane of the objective at the photodiodes.

Optical measurements

The experimental chamber was mounted on the rotating stage of a modified polarizing microscope. The muscle fiber was illuminated with light from an He-Ne laser polarized at 45° to the fiber axis (Fig. 1). The fiber birefringence introduces a phase lag—the retardation, ϕ—between components of the light polarized parallel and perpendicular to the fiber axis. The retardation is equal to the birefringence multiplied by the optical path length in the fiber. The quarter-wave plate converts this phase difference into an intensity difference between the parallel and perpendicular components, which are separated by a Wollaston prism so that their intensities can be measured with photodiodes. The difference divided by the sum of the photodiode outputs (R, calculated electronically) is equal to the sine of the retardation phase angle ϕ (Taylor and Zeh, 1976). A retardation compensator was also used to measure steady-state retardation by a null method in which the fiber was viewed between crossed polarizers by replacing the quarter-wave plate with an analyser (Peckham and Irving, 1989).

For continuous measurements of retardation the method of Irving (1993) was used. Fibers were illuminated by a beam that was ~0.7 mm long and 45–80% wider than the fiber segment to minimize movement artifacts. Fiber transmittance (T, the fraction of the light incident on the fiber that is transmitted by it and collected by the objective) was measured from the ratio of the sum of the photodiode outputs with the fiber in and out of the illuminating beam. T was 0.75 ± 0.02 (mean ± SE, seven fibers) in relaxing solution at sarcomere length 2.8–2.9 μm. There was no significant change in T after putting fibers into rigor. Fiber dichroism was negligible, as in the case of intact frog fibers with the same optical setup (Irving, 1993). The retardation at the thickest part of the fiber, ϕ_c, was calculated assuming that the fiber cross-section was elliptical. In this case

$$R = (1 - g)S - g \cdot \sin\theta$$

where

$$S = \pi/2 \cdot J_1(\phi_c)\cos\theta - [1 - \pi/2 \cdot H_1(\phi_c)]\sin\theta,$$

and J_1 and H_1 are, respectively, Bessel and Struve functions of first order; θ is the retardation introduced by the compensator; and g is $f/[(1 - f)T + f]$, where f is the fraction of the light in the illuminating beam that bypasses the fiber (Irving, 1993). The value of ϕ_c predicted from the above equations and measurements of R, θ, f and T was not significantly different from that measured directly by the visual compensator null method. The ratio of ϕ_c values determined by the two methods was 0.99 ± 0.03 (mean ± SE, seven fibers), showing that the assumption of elliptical cross-section does not produce significant error. All retardation measurements were corrected for the small background value caused by the birefringence of the apparatus. The fractional change in retardation is equal to that in R for small changes around the null point (Irving, 1993). For continuous measurement of changes in retardation, the time course of the change in retardation was therefore assumed to be equal to that in R.

The optical path length in the fiber was not measured in the present series of experiments. Initial values of birefringence (retardation divided by optical path length) in relaxing solution were estimated assuming that optical path length d was equal to fiber width w, and these estimates agreed with results of previous studies in which optical path length was measured (see Results).

Relative changes in birefringence can be determined without measuring optical path length. In the general case in which changes in birefringence

may be caused by changes in either fiber volume or protein orientation, the effects of volume changes can be eliminated by calculating a "standard birefringence, $B^{o''}$ at a standard fiber volume (Peckham and Irving, 1989). The calculation assumes that, in the absence of orientation changes, birefringence is inversely proportional to fiber volume (Fredericq and Houssier, 1973; Peckham and Irving, 1989). If the optical path length d changes from d_1 to d_2 and fiber width from w_1 to w_2 the ratio of fiber volumes would be w_2d_2/w_1d_1 under the assumption of elliptical cross-section. Thus the ratio of standard birefringence values in two different conditions, B^o_2/B^o_1, is given by $B_2w_2d_2/B_1w_1d_1 = \phi_2w_2/\phi_1w_1$ (where B_1 and B_2 are the observed birefringence values, and ϕ_1 and ϕ_2 are the observed values of ϕ_c), and the relative change in standard birefringence is independent of optical path length. Steady-state changes in relative standard birefringence were calculated from measurements of ϕ_c and w using this relation.

This method was not used for continuous measurement of standard birefringence because fiber width was not recorded continuously. Changes in fiber volume and cross-sectional shape were small under the experimental conditions used here. The ionic strength and composition of the solutions (Table 1) were chosen so that the change in filament lattice spacing associated with the rigor/relaxed transition was less than 1% (Brenner et al., 1984; Ferenczi et al., 1987; Peckham and Irving, 1989). Changes in fiber shape were minimized by careful mounting of the fibers in the T-clips and stretching to a mean sarcomere length of 2.8–2.9 μm before putting them into rigor. Fibers that twisted or showed transverse movement or width change on going into rigor were rejected. In the fibers used for the photolysis experiments fiber width in relaxing and rigor solutions differed by less than 2% (Table 2). If this were caused by a systematic change in fiber shape at constant volume the error in the intensity ratio R in the wide-field illumination method used here would be 0.2% (see Fig. 13C in Irving, 1993), which is negligible. It was therefore assumed that R was proportional to standard birefringence throughout the relaxation transients, and the R signals were calibrated using the pre- and post-photolysis steady-state measurements of standard birefringence made by the method described in the preceding paragraph.

Photolysis experiments

Fibers were mounted in relaxing solution at 15°C. The sarcomere length was set to 2.8–2.9 μm, measured with a 40×, 0.65N.A. objective. This was then exchanged for a 10×, 0.22N.A. objective, and the retardation at the thickest part of the fiber cross-section, ϕ_c, was measured by the compensator null method, viewing the fiber between crossed polarizers. Fiber width and the width of the illuminating light beam were recorded. The quarter-wave plate was inserted, and the intensity ratio R and transmittance T were determined; then the compensator retardation θ was set to give $R = 0$. The fiber was put into rigor solution (Table 1) and after rigor tension had developed the fiber width was measured again. The compensator was renulled and the new value of θ used to calculate the retardation change. Fibers were then incubated in caged ATP solution (Table 1) for at least 2 min. Caged ATP was photolysed by a 30–50 mJ pulse of wavelength 320 nm from a frequency-doubled dye laser (Candela SLL 1050, Natick, Mass.), focused at the chamber by a fused silica cylindrical lens. An Oriel 5181 filter (Oriel Corp., Stratford, CT) was used to absorb the primary light emitted by the laser. To minimize flash artifacts adjustable masks were used to prevent the laser pulse illuminating the motor and transducer hooks. The gain of the photodiode amplifiers was reduced during the flash and the preflash outputs transiently maintained by sample-and-hold circuits. After relaxation was complete (~1 s) the fiber width was measured and the compensator renulled. A solution sample was taken from the experimental chamber and analyzed for nucleotide and caged nucleotide concentrations by reverse-phase high-performance liquid chromatography (Merck RP8 column with 10 mM KH_2PO_4, pH 5.5, 10% methanol). On average 1.35 ± 0.05 mM MgATP (mean ± SE, n = 16) was released by a single flash. Finally optical measurements (null θ, f and w) were made in the standard relaxing solution.

TABLE 2 Width and birefringence changes between relaxing and rigor conditions

	Relaxed to rigor solution	Relaxation, 1 s after photolysis of caged ATP
Width	−1.8 ± 1.1%	+1.9 ± 0.5%
Retardation	−4.4 ± 1.4%	+4.1 ± 0.7%
Standard birefringence	−5.7 ± 1.0%	+5.8 ± 0.7%

Percentage change in fiber width, retardation, and standard birefringence (expressed relative to the relaxed values) on the initial transfer from relaxing to rigor solution (first column) and 1 s (second column) after photolysis of caged ATP. Mean ± SE from six fibers. Retardation and birefringence values in the second column were determined from the change in R during the flash, using the width measured less than 1 min after relaxation (see Materials and Methods). Compensator null values at this time gave fractional changes in retardation and standard birefringence of 5.1 ± 2.2% and 7.1 ± 2.2%, respectively.

Stiffness measurements

Instantaneous stiffness was measured on the same set-up by applying stretches of ~7 nm/half sarcomere complete in ~200 μs to the rigor fiber or at various times after release of ATP (see Fig. 3). The movement at the motor hook was measured with a vane and differential photodiode detector and the motor position signal corrected as described by Goldman and Simmons (1986). The response of the force transducer was determined at the end of each experiment using a nylon monofilament connection attached via T-clips between the motor and transducer. The natural frequency of the transducer was 2.9 kHz and the damping time constant typically 0.1 ms. The force transducer records were corrected as described by Ford et al. (1977). Instantaneous force/length plots were made from the corrected traces, and these were linear during most of the length change for the nylon monofilament or a rigor muscle fiber (Fig. 3 *B*). Instantaneous stiffness was determined from the linear portion of these force/length plots.

RESULTS

In relaxing solution at sarcomere length 2.8–2.9 μm the birefringence, calculated assuming that optical path length is equal to fiber width, was 2.05 ± 0.09 × 10^{-3} (mean ± SE, n = 6). This is similar to the value previously reported for the same solution at sarcomere length 2.4 μm (2.14 ± 0.02 × 10^{-3}; see Table 2 in Peckham and Irving, 1989). The birefringence decreased when muscle fibers were put into rigor (Table 2). After correction for a small reduction in width the decrease in standard birefringence was 5.7 ± 1.0%, which may be compared with 7.4 ± 0.8% determined previously at sarcomere length 2.4 μm (Peckham and Irving, 1989). The smaller decrease at the longer sarcomere length used here is expected from the reduction in filament overlap (Peckham and Irving, 1989). No further change in width or birefringence was observed when the rigor solution was exchanged for one containing caged ATP.

When about 1 mM ATP was released by laser flash photolysis of caged ATP the birefringence returned to its relaxed value (Table 2, Fig. 2). Following the photolysis pulse and associated flash artifact there was a lag of 50–100 ms before tension began to fall (Fig. 2). The half-time for tension relaxation, measured from the time of the flash, was 202 ± 15 ms (n = 6). The slower relaxation compared to previous reports (Goldman et al., 1984) is due to both the lower ionic strength (100 mM) and temperature (15°C) used in the experiments presented in Fig. 2. When the ionic strength and temperature were raised to 200 mM and 20°C respectively, relaxation half-times were in the range 50–100 ms.

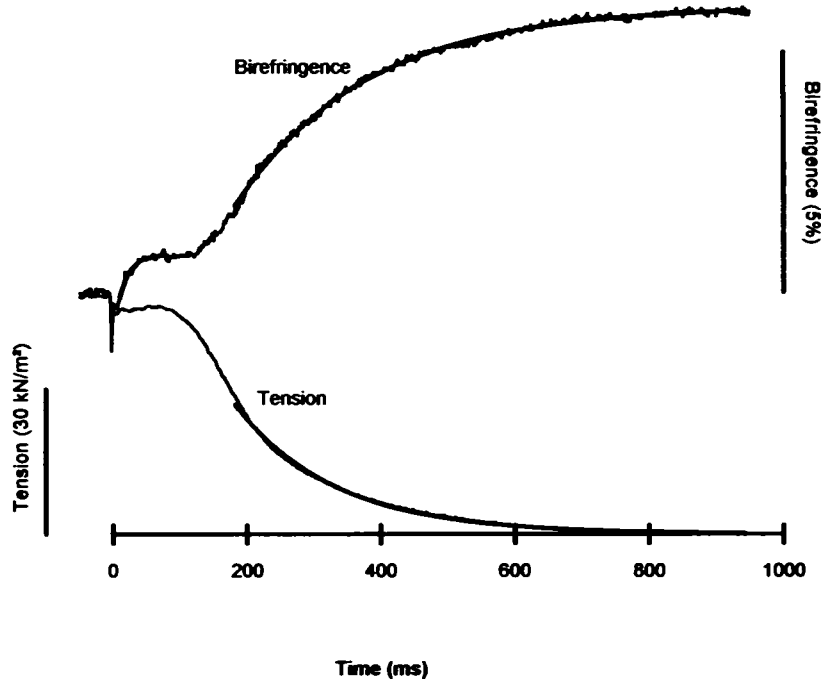

FIGURE 2 Birefringence and tension changes accompanying relaxation produced by photolysis of caged ATP. Each trace is averaged from the six fibers in Table 1. The birefringence traces were obtained by scaling the ratio R to the final standard birefringence change for each fiber after photolysis (see Materials and Methods and Table 1), and the calibration bar also refers to standard birefringence. Tension/cross-sectional area was estimated from fiber width by assuming width was equal to depth. The laser flash occurs at time 0. The three smooth lines are least-squares fits to a single exponential for the portion of the trace for which each fit is shown.

After ATP release birefringence increased in two distinct phases separated by a period of ~50–100 ms after ATP release when birefringence was almost constant (Fig. 2). The initial rapid increase was small, corresponding to only a 0.9 ± 0.2% change in standard birefringence (mean ± SE, n = 6) but was observed in all fibers. This phase of the birefringence increase was reasonably well fit by an exponential with a rate constant of 63 s^{-1} (Fig. 2). The slower phase of the birefringence increase was much larger, corresponding to a 4.9 ± 0.7% change in standard birefringence. An exponential fit to this region gave a rate constant of 5.1 s^{-1}, which was slightly slower than the rate constant determined by fitting the final force relaxation, 6.7 s^{-1} (Fig. 2). The half-time for the overall increase in birefringence was 267 ± 31 ms (n = 6), which is slightly greater than the corresponding value for the tension relaxation (202 ± 15 ms), although the paired difference was not significant at the 5% level.

We also attempted to measure birefringence transients during development of active contraction induced by ATP release in the presence of calcium using a caged ATP solution like that in Table 1 except that EGTA was replaced by CaEGTA. The observed retardation changes were much smaller than those seen on relaxation, but contained slow components of variable polarity that may be related to longitudinal translation of sarcomeres during activation. We therefore did not attempt to characterize the underlying birefringence changes. Force development in these conditions was well fitted, after an initial lag phase, by a single exponential with rate constant 14.4 ± 1.4 s^{-1} (mean ± SE, n = 14).

Stiffness measurements

The birefringence results presented above (Fig. 2) suggest that a small structural change occurred during the first 50 ms after ATP release, when tension was roughly constant, and a larger change accompanied the final mechanical relaxation. In an attempt to find a mechanical correlate for the faster process, we measured fiber stiffness in the conditions used for the birefringence measurements. Rapid stretches were applied at different times after the laser flash, and the tension responses compared with those observed in relaxing and rigor conditions (Fig. 3). Already at 10 ms after ATP release fiber stiffness was reduced compared with the rigor value. Moreover, in contrast with the behavior in rigor, at 10 ms after ATP release tension did not remain constant after the stretch, but recovered on the millisecond time scale (Fig. 3 *A*). These results show that the characteristic mechanical properties of rigor muscle are lost rapidly after ATP release despite the lag in mechanical relaxation.

The time course of the change in instantaneous stiffness after ATP release was determined in more detail from the tension/length plots obtained during the length steps (Fig. 3 *B*). Instantaneous stiffness fell rapidly to about half its rigor value in the first 50 ms after ATP release (Fig. 4). An exponential fit to the points in this time range gave a rate constant of 43 s^{-1}, which is similar to that of the initial birefringence increase of 63 s^{-1}. This fast component was much more prominent in instantaneous stiffness (Fig. 4) than in birefringence (Fig. 2). Stiffness, like birefringence, also shows a slow component (Fig. 4), which was not studied in detail.

To obtain an approximate estimate of the extent of the rapid (~1000 s^{-1}) recovery process after a stretch, the tension recovery 1.7 ms after the stretch ($T_1-T_{1.7\ ms}$, where T_1 is the tension at the end of the stretch and $T_{1.7\ ms}$ is the tension 1.7 ms later) was expressed as a fraction of the peak tension change during the stretch (T_1-T_0, where T_0 is the tension before the stretch). The quantity $(T_1-T_{1.7\ ms})/(T_1-T_0)$ increased rapidly after ATP release, and an exponential fit to

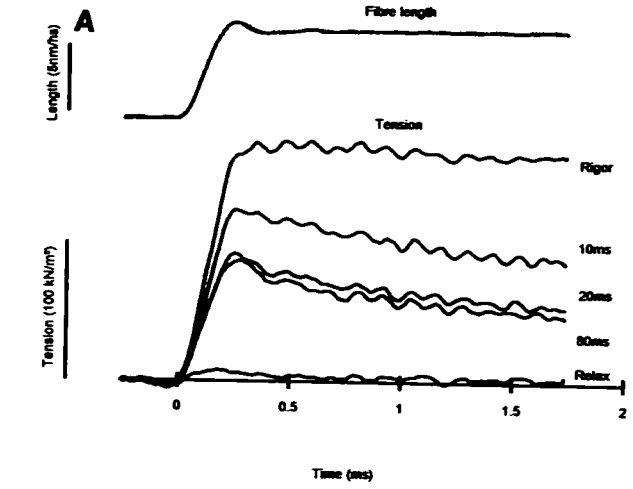

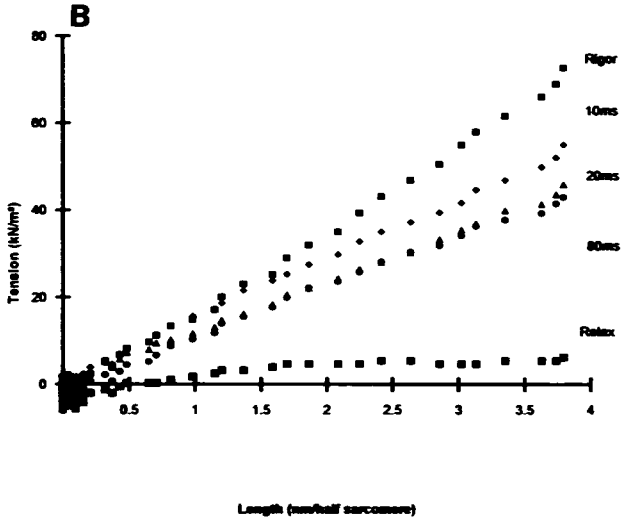

FIGURE 3 (*A*) Fiber length and tension changes accompanying stretches of relaxed and rigor fibers, and 10, 20, and 80 ms after photolysis of caged ATP. The tension traces have been shifted vertically to superimpose before application of the length step. Length and tension signals were corrected for motor and transducer characteristics as described in Materials and Methods. (*B*) Instantaneous tension-length plots during the length steps, from the data in (A). The slope of these plots gives a measure of instantaneous stiffness.

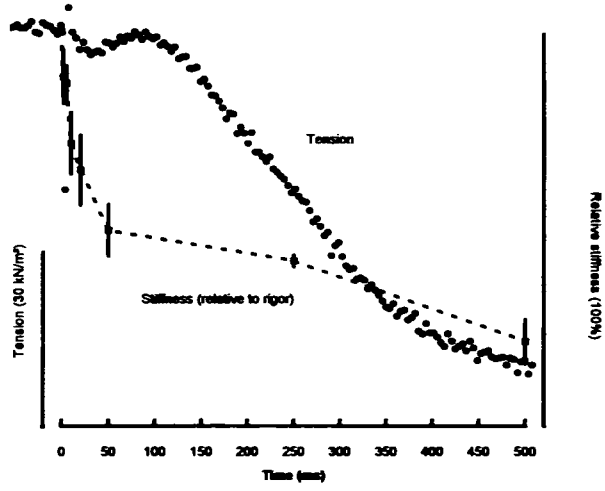

FIGURE 4 Instantaneous stiffness (■) and tension (●) accompanying relaxation produced by photolysis of caged ATP. The stiffness measurements were made as in Fig. 3 and scaled to the rigor value after subtracting the relaxed stiffness, which at this sarcomere length was 0.198 ± 0.026 (mean ± SE, $n = 6$) of that in rigor. The error bars on the stiffness values show SE for 3,2,4,4,3,4, and 2 fibers. The tension trace is averaged from the six fibers used in this protocol.

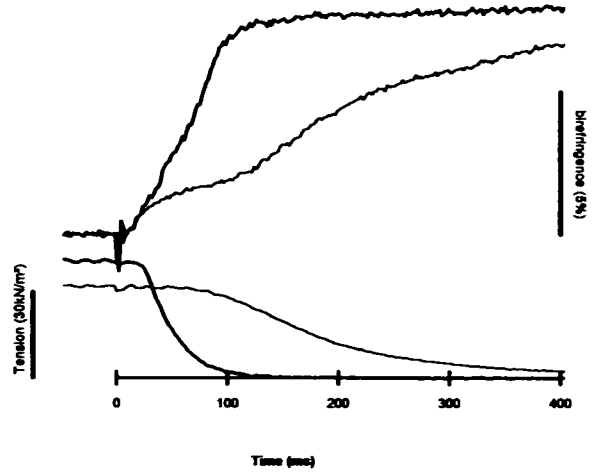

FIGURE 5 Birefringence and tension changes accompanying relaxation produced by photolysis of caged ATP in the presence (*thicker traces*) and absence (*thinner traces*) of 10 mM phosphate. Three fibers were used; the traces in the presence of phosphate are the average of three records and those in the absence of phosphate the average of five (three before and two after the phosphate records were obtained).

the points from the first 50 ms gave a rate constant of 126 s^{-1}. The rapid tension recovery process seems to develop more rapidly after ATP release than either the decrease in instantaneous stiffness or the increase in birefringence.

Effect of inorganic phosphate

Phosphate accelerates mechanical relaxation after photolysis of caged ATP (Hibberd et al., 1985), presumably by binding to the actomyosin.ADP intermediate formed after hydrolysis. Thus phosphate is a useful tool for correlating the mechanical and structural signals with biochemical transitions. In the present conditions 10 mM phosphate decreased the lag preceding tension relaxation (Fig. 5) and increased the final rate of relaxation by a factor of about 4 (Table 3). The birefringence transient was likewise accelerated so that the change in both signals was almost complete 100 ms after ATP release (Fig. 5). The overall half-time of the birefringence change was slightly greater than that of tension, and the rate constant of an exponential fit to the final part of each trace was smaller (Table 3). In the presence of 10 mM phosphate the fast and slow components of the birefringence change could no longer be clearly separated. However, phosphate had little effect on either force or birefringence in the first 20 ms after ATP release, when the fast birefringence signal was well underway.

TABLE 3 Effect of 10 mM phosphate

	No phosphate	10 mM phosphate
Relaxing to rigor solution, $\Delta\beta°$	−7.2 ± 0.8%	−4.2 ± 0.5%
Relaxation by caged ATP photolysis, $\Delta\beta°$	8.1 ± 3.0%	7.9 ± 1.7%
Half-time of overall tension change (ms)	186 ± 15	43.5 ± 1.9
Half-time of overall birefringence change (ms)	201 ± 11	69.9 ± 15.0
Rate constant of final tension relaxation (s^{-1})	9.3	38.8
Rate constant of final birefringence change (s^{-1})	6.1	23.1

Change in standard birefringence $\Delta\beta°$, half-times and final rates of tension and birefringence changes from the three fibers used for Fig. 5. Standard birefringence changes calculated as in Table 2. Values for no phosphate are means of five traces, three of which were before the photolysis trials with phosphate and the other two after. Values for 10 mM phosphate are means of three traces. The standard birefringence change for relaxing to rigor solution seemed to be smaller in the presence than in the absence of phosphate, but this difference is probably not real, as the changes produced by caged ATP photolysis were similar in the two cases. The rate constants were obtained from exponential fits to the average traces with and without phosphate.

DISCUSSION

Origin of the birefringence signals

Following ATP release in a rigor muscle fiber in the absence of calcium the standard birefringence increased by 5.8 ± 0.7% (Table 2, Fig. 2). A decrease in birefringence of similar magnitude was observed when the fibers were transferred from relaxing to rigor solution (5.7 ± 1.0%, Table 2), which is consistent with previous steady-state measurements (Peckham and Irving, 1989). Inasmuch as the filament lattice spacing is the same in these two solutions (Ferenczi et al., 1987; Peckham and Irving, 1989), the increase in birefringence after ATP release must be caused by a change in orientation of filament components rather than a change in the fraction of the fiber volume occupied by filaments. As in the case of the previous steady-state measurements, we conclude that the birefringence increase after ATP release is caused by an increase in the average degree of alignment of myosin heads with the fiber axis.

The time course of the birefringence increase showed a small fast phase during the first 50 ms after ATP release and a larger slow phase over about the next 1 s (Fig. 2). Although the amplitude of the fast phase was small, 0.9 ± 0.2% change in standard birefringence, it was the most reproducible part of the birefringence transient, as indicated by the small standard error. This reproducibility is likely to be caused by the presence of residual rigor attachments, preventing changes in the cross-sectional shape of the fibers. For the same reason redistribution of sarcomere length is unlikely to have occurred in this period (see Fig. 8 in Dantzig et al., 1991). The force in the fiber was almost constant, so the length of series elastic structures would not have changed. Therefore the small fast component of the birefringence increase is unlikely to be caused by a systematic movement artifact. Time-resolved x-ray diffraction measurements showed no transient change in filament lattice spacing during this period (Ferenczi et al., 1987). Therefore the fast increase in birefringence, like the larger slower component, is likely to be caused by an increase in the average degree of alignment of myosin heads with the fiber axis.

Relation of the birefringence changes to transitions in the actomyosin ATPase cycle

The fast birefringence component is likely to be associated with the formation of myosin.ATP and myosin.ADP.Pi states, which are weakly bound to actin. In the conditions used here the rate of ATP release from caged ATP is 100 s^{-1} (Barabas and Keszthelyi, 1984). The second-order rate constant for ATP binding to actomyosin is 1–4 × 10^6 M^{-1} s^{-1} for the proteins in solution at ionic strength 0.1 M, pH 7.0, 20°C (White and Taylor, 1976). Thus, when 1 mM ATP is released from caged ATP in the presence of ~0.15 mM myosin heads, the formation of the actomyosin.ATP complex is expected to occur at a rate greater than 100 s^{-1} (Goldman et al., 1984). ATP hydrolysis occurs at ~60 s^{-1} in rabbit psoas fibers at ionic strength 0.2 M, 12°C (Ferenczi, 1986), and the rate in solution at ionic strength 0.1 M, 15°C can be estimated as ~80 s^{-1} from the data of Johnston and Taylor (1978). Thus, at the end of the fast birefringence component with rate 63 s^{-1}, the intermediates AM.ATP and AM.ADP.Pi (where A represents actin and M myosin) are likely to be present. Given that myosin is weakly and reversibly bound to actin in these states (Stein et al., 1979), they are likely to be in rapid equilibrium with the detached states M.ATP and M.ADP.Pi. Consistent with these conclusions, the fast birefringence component is well underway before significant effects of phosphate can be detected in either the birefringence or force traces (Fig. 5), suggesting that phosphate release has not yet taken place.

Changes in mechanical properties following ATP release

The changes in mechanical properties of the muscle fibers during the fast birefringence component were studied by imposing step stretches at various times after ATP release. Because of restrictions imposed by the optical apparatus, these measurements were made with relatively long, non-coaxial hooks on the motor and transducer. This introduced some undesired oscillations in the tension transients (Fig. 3), but should not have affected measurements of relative changes in mechanical characteristics of the fibers in the first 50 ms after the flash, when force and series elastic extension are constant. Furthermore, the presence of some residual rigor crossbridges in this period is likely to prevent redistribution of sarcomere length, as argued above. By the end of the fast phase of the birefringence increase, instantaneous stiffness had fallen to about half its rigor value (Fig. 4), and there was a rapid component of force recovery after a step stretch (Fig. 3). The fitted rate constants of 43 s^{-1} for the change in instantaneous stiffness and 126 s^{-1} for the onset of the fast force

recovery process are similar but not identical to that of the birefringence fast phase, 63 s^{-1}. These mechanical changes are qualitatively consistent with the formation of AM.ATP and AM.ADP.Pi states in rapid equilibrium with their detached counterparts, but might also indicate the presence of actively cycling crossbridges soon after ATP release. A more extensive mechanical investigation would be required to distinguish between these possibilities.

It is perhaps surprising that the isometric force borne by the fiber is virtually constant during the fast birefringence component and the accompanying stiffness decrease (Figs. 2 and 4). The observation that mechanical relaxation is slower than the initial detachment of myosin heads from actin suggests that these rapidly detaching heads either were unstrained in the rigor fiber, or can reattach and regenerate the original force even in the absence of calcium, at least until the cooperative activation of the thin filament in the rigor state is overcome (Goldman et al., 1984). Because active force generation is slower than detachment, the simplest models based on the latter hypothesis would predict a transient dip in force. Such a force dip is very small or absent in the present conditions (Figs. 2 and 4), despite the relatively slow rate of active force development observed in the presence of calcium, 14.4 s^{-1}. Another possible explanation for the maintained force is that a fraction of the myosin heads may have bound contaminant ADP before the laser flash (Sleep and Burton, 1990; Thirlwell et al., 1993). These heads would release ADP slowly and may make a disproportionate contribution to the recorded force (Dantzig et al., 1991) but may not contribute to the fast component of the birefringence change.

Changes in myosin head orientation after ATP release

Birefringence is sensitive to the average degree of alignment of the myosin heads with the fiber axis. If all the heads had the same orientation, the angle between the long axis of the myosin heads and the fiber axis would be ~50° in rigor and ~30° in relaxing conditions (Peckham and Irving, 1989). The amplitude of the fast birefringence component is only about 15% of the total increase between rigor and relaxing conditions (Fig. 2), corresponding to an increase in axial angle of only a few degrees in this simple model. However, the birefringence would not be sensitive to a transition from the rigor angle to a wide degree of orientational disorder, because the rigor angle is close to the angle (54.7°), which gives the same birefringence as an isotropic distribution. Thus the fast birefringence component indicates a small increase in the average degree of alignment of the long axis of the heads with the filament axis, which may be accompanied by a large increase in the disorder of head orientations.

The possible states of the myosin head at the end of the fast component can be grouped as follows: 1) residual rigor heads (or AM.ADP heads), 2) weakly attached AM.ATP or AM.ADP.Pi heads and their detached counterparts M.ATP and M.ADP.Pi, 3) actively cycling heads, and 4) detached heads in the equilibrium-relaxed configuration.

The fraction of the myosin heads in each group of states is unknown. However, the birefringence for each group can be estimated from previous steady-state measurements. Group 2 (AM.ATP, AM.ADP.Pi, M.ATP, M.ADP.Pi) is also present in low ionic strength relaxing conditions (Brenner et al., 1982). The birefringence in low ionic strength relaxing solution is close to the rigor value (Peckham and Irving, 1989) and not significantly different from that at the end of the fast birefringence component reported above. The birefringence in active contraction is also close to that in rigor (Irving, 1993), but the birefringence in equilibrium-relaxed fibers at physiological ionic strength is much higher than in the other steady states (Peckham and Irving, 1989) and indeed is the value reached at the end of the slow birefringence component (Table 2). Thus the birefringence soon after ATP release, at the end of the fast component, is consistent with the presence of either weakly attached or actively cycling crossbridges (as well as some residual rigor heads), but not with a large fraction of myosin heads being in the equilibrium-relaxed configuration.

The large slow birefringence component, on the other hand, does indicate a large increase in the average alignment of the long axis of the myosin heads with the fiber axis. This suggests that the equilibrium-relaxed configuration is achieved with a time course similar to that of the final mechanical relaxation.

Comparison with the results of other structural methods

Fast myosin movements induced by photolytic ATP release in the absence of calcium in rabbit psoas fibers have been demonstrated previously by other structural methods. In each case the structural change significantly preceded mechanical relaxation. The intensities of the equatorial x-ray reflections, which are sensitive to the distribution of mass between the actin and myosin filaments, change with a rate constant of ~300 s^{-1} at 10–12°C, and pH 6.8 (Poole et al., 1991). The polarization of fluorescence from rhodamine probes bound to myosin light chain 2 changes with a rate constant of ~100 s^{-1} at ionic strength 0.2 M, pH 7.0, 20°C (Allen et al., 1992). The difference between these rate constants and that of the fast birefringence component (63 s^{-1}) might be caused by either the different experimental conditions or the sensitivity of the structural methods to different types of motion of the myosin head and its constituent domains.

These structural methods probably do report different types of motion, as the birefringence signal is dominated by a large slow component (Fig. 2), whereas both the equatorial x-ray diffraction (Poole et al., 1991) and myosin light chain fluorescence signals (Allen et al., 1992) are dominated by the fast component. Such qualitative differences between the signals are unlikely to be caused by the different solution conditions.

The x-ray and light chain fluorescence signals described above suggest that the fraction of heads remaining in rigor at the end of the fast component is small. The light chain fluorescence signal shows that the light chain domain of the

head is rapidly disordered after ATP release. The disorder may extend to the whole of the head, given that electron paramagnetic resonance studies of fibers labeled with spin probes on the reactive sulphydryl of the myosin heavy chain show dynamic disorder both in low ionic strength relaxing conditions (Fajer et al., 1991) and during active contraction (Fajer et al., 1990; Berger and Thomas, 1993). The conformation of the myosin heads in these steady-state measurements is likely to be similar to that soon after ATP release, as argued above, and is therefore consistent with substantial disorder of head orientations at this time. A difference in the degree of head disorder between low and normal ionic strength relaxing conditions was also demonstrated by Fajer et al. (1991), consistent with the birefringence difference between these states (Peckham and Irving, 1989).

We thank T. Rutherford and K. Eason for technical support and R.M. Simmons, J.A. Sleep and D.R. Trentham for helpful comments on an earlier version of the manuscript.

This work was supported by the Medical Research Council, the Wellcome Trust, and the Royal Society (U.K.). M. P. was a postdoctoral fellow of the Muscular Dystrophy Association (U.S.A.).

REFERENCES

Allen, T. S., N. Ling, Y. E. Goldman, and M. Irving. 1992. Structural changes of myosin light chain 2 in skinned muscle fibers following photolysis of caged ATP and ADP. *Biophys. J.* 61:A286.

Barabas, K., and L. Keszthelyi. 1984. Temperature dependence of ATP release from "caged ATP." *Acta Biochim. Biophys. Acad. Sci. Hungary.* 19:305–309.

Berger, C. L., and D. D. Thomas. 1993. Rotational dynamics of actin-bound myosin heads in active myofibrils. *Biochemistry.* 32:3812–3821.

Brenner, B., M. A. Ferenczi, M. Irving, R. M. Simmons, and E. Towns-Andrews. 1989. Myosin crossbridge movement observed by time-resolved X-ray diffraction in a single permeabilised fiber isolated from frog muscle. *J. Physiol.* 415:113P.

Brenner, B., M. Schoenberg, J. M. Chalovich, L. E. Greene, and E. Eisenberg. 1982. Evidence for cross-bridge attachment in relaxed muscle at low ionic strength. *Proc. Natl. Acad. Sci.* 79:7288–7291.

Brenner, B., L. C. Yu, and R. J. Podolsky. 1984. X-ray diffraction evidence for cross-bridge formation in relaxed muscle fibers at various ionic strengths. *Biophys. J.* 46:299–306.

Dantzig, J. A., M. G. Hibberd, D. R. Trentham, and Y. E. Goldman. 1991. Cross-bridge kinetics in the presence of MgADP investigated by photolysis of caged ATP in rabbit psoas muscle fibers. *J. Physiol.* 432: 639–680.

Fajer, P. G., E. A. Fajer, M. Schoenberg, and D. D. Thomas. 1991. Orientational disorder and motion of weakly attached cross-bridges. *Biophys. J.* 60:642–649.

Fajer, P. G., E. A. Fajer, and D. D. Thomas. 1990. Myosin heads have a broad orientation distribution during isometric muscle contraction: time-resolved EPR studies using caged ATP. *Proc. Natl. Acad. Sci.* 87: 5538–5542.

Ferenczi, M. A. 1986. Phosphate burst in permeable muscle fibers of the rabbit. *Biophys. J.* 50:471–477.

Ferenczi, M. A., R. S. Goody, M. Irving, Y. Maeda, M. Peckham, K. J. V. Poole, and G. Rapp. 1987. Time-resolved measurements of filament lattice spacing in rabbit psoas muscle fibers following rapid photogeneration of ATP from caged-ATP. *Biophys. J.* 51:470a.

Ferenczi, M. A., M. Irving, and M. Peckham. 1986. Birefringence transients during relaxation of demembranated rabbit muscle fibers from rigor following laser flash photolysis of caged-ATP. *J. Physiol.* 381:86P.

Ford, L. E., A. F. Huxley, and R. M. Simmons. 1977. Tension responses to sudden length change in stimulated frog muscle fibers near slack length. *J. Physiol.* 269:441–515.

Fredericq, E., and C. Houssier. 1973. Electric Dichroism and Electric Birefringence. Clarendon Press, Oxford.

Goldman, Y. E. 1987. Kinetics of the actomyosin ATPase in muscle fibers. *Annu. Rev. Physiol.* 49:637–654.

Goldman, Y. E., M. G. Hibberd, J. A. McCray, and D. R. Trentham. 1982. Relaxation of muscle fibers by photolysis of caged ATP. *Nature* 300: 701–705.

Goldman, Y. E., M. G. Hibberd, and D. R. Trentham. 1984. Relaxation of rabbit psoas muscle fibers from rigor by photogeneration of adenosine-5′-triphosphate. *J. Physiol.* 354:577–604.

Goldman, Y. E., and R. M. Simmons. 1986. The stiffness of frog skinned muscle fibers at altered lateral filament spacing. *J. Physiol.* 378:175–194.

Haskell, R. C., F. D. Carlson, and P. S. Blank. 1989. Form birefringence of muscle. *Biophys. J.* 56:401–413.

Hibberd, M. G., J. A. Dantzig, D. R. Trentham, and Y. E. Goldman. 1985. Phosphate release and force generation in skeletal muscle fibers. *Science* 228:1317–1319.

Hibberd, M. G., and D. R. Trentham. 1986. Relationship between chemical and mechanical events during muscular contraction. *Annu. Rev. Biophys. Biophys. Chem.* 15:119–161.

Hirose, K, T. D. Lenart, J. M. Murray, C. Franzini-Armstrong, and Y. E. Goldman. 1993. Flash and smash: rapid freezing of muscle fibers activated by photolysis of caged ATP. *Biophys. J.* 65:397–408.

Irving, M. 1993. Birefringence changes associated with isometric contraction and rapid shortening steps in frog skeletal muscle fibers. *J. Physiol.* 472:127–156.

Irving, M., M. Peckham, and M. A. Ferenczi. 1988. Birefringence as a probe of crossbridge orientation in demembranated muscle fibers. *In* Molecular Mechanism of Muscle Contraction, H. Sugi and G. H. Pollack, editors. Plenum Publishing Corp., New York. 299–306.

Johnston, K. A., and E. W. Taylor. 1978. Intermediate states of subfragment-1 and acto-subfragment-1 ATPase: reevaluation of the mechanism. *Biochemistry.* 17:3432–42.

Peckham, M., and M. Irving. 1989. Myosin crossbridge orientation in demembranated muscle fibers studied by birefringence and X-ray diffraction measurements. *J. Mol. Biol.* 210:113–126.

Poole, K. J. V., Y. Maeda, G. Rapp, and R. S. Goody. 1991. Dynamic x-ray diffraction measurements following photolytic relaxation and activation of skinned rabbit psoas fibers. *Adv. Biophys.* 27:63–75.

Poole, K. J. V., G. Rapp, Y. Maeda, and R. S. Goody. 1988. The time course of changes in the equatorial diffraction patterns from different muscle types on photolysis of caged ATP. *In* Molecular Mechanism of Muscle Contraction, H. Sugi and G. H. Pollack, editors. Plenum Publishing Corp., New York. 391–401.

Sleep, J., and K. Burton. 1990. The use of apyrase in caged ATP experiments. *Biophys. J.* 57:542a.

Stein, L. A., R. P. Schwarz, P. B. Chock, and E. Eisenberg. 1979. Mechanism of actomyosin adenosine triphosphatase. Evidence that adenosine-5′-triphosphate hydrolysis can occur without dissociation of the actomyosin complex. *Biochemistry.* 18:3895–3909.

Tanner, J. W., D. D. Thomas, and Y. E. Goldman. 1992. Transients in orientation of a fluorescent cross-bridge probe following photolysis of caged nucleotides in skeletal muscle fibers. *J. Mol. Biol.* 223:185–203.

Taylor, D. L. 1976. Quantitative studies on the polarisation optical properties of striated muscle. I. Birefringence changes of rabbit psoas muscle in the transition from rigor to relaxed state. *J. Cell Biol.* 68:497–511.

Taylor, D. L., and R. M. Zeh. 1976. Methods for the measurement of polarisation optical properties. I. Birefringence. *J. Microsc.* 108:251–259.

Thirlwell, H., F. Bancel, and M. A. Ferenczi. 1993. Relaxation of rigor tension by photolysis of caged ATP in permeabilized muscle fibers of the rabbit. *Biophys. J.* 64:A251.

White, H. D., and E. W. Taylor. 1976. Energetics and mechanism of actomyosin adenosine triphosphatase. *Biochemistry.* 15:5818–26.